Chemistry Faculty Publications   Chemistry Department

5-2-1995

Electrochemical Carbonylation of Organoiron Methyl Complex: A Study of Reaction Intermediates

C. Amatore
Ecole Normale Superieure

Mekki Bayachou
Cleveland State University, M.BAYACHOU@csuohio.edu

J. N. Verpeaux
Ecole Normale Superieure

L. Pospisil
Institute of Physical Chemistry

J. Fiedler
Institute of Physical Chemistry

Recommended Citation

Amatore, C.; Bayachou, Mekki; Verpeaux, J. N.; Pospisil, L.; and Fiedler, J., "Electrochemical Carbonylation of Organoiron Methyl Complex: A Study of Reaction Intermediates" (1995). *Chemistry Faculty Publications*. 310.

https://engagedscholarship.csuohio.edu/scichem_facpub/310

Electrochemical carbonylation of organoiron methyl complex: a study of reaction intermediates

C. Amatore , M. Bayachou   J.-N. Verpeaux , L. Pospíšil   J. Fiedler

Abstract

The one-electron reduction of CpFe(CO)$_2$CH$_3$ has been investigated by voltammetry and Fourier transform IR spectroelectrochemistry. The reduction initiates the insertion of CO ligand in the Fe–CH$_3$ bond. The dissociation of a CO group proceeds in a parallel reaction. Reaction intermediates, the acyl derivative and released CO, form the radical anion of a complex CpFe(CO)$_2$(COCH$_3$) which is able to reduce the parent compound. The reversible redox potential -1.8 V of CpFe(CO)$_2$(COCH$_3$) allows the regeneration of its radical anion which drives a catalytic cycle. The lifetime of intermediates is shortened by side reactions, one of which is the migration of the acyl group from the central atom to the cyclopentadienyl ring. This explains the apparent discrepancy between products observed in preparative scale electrolysis and the absence of catalytic effects in routine voltammetric experiments.

Keywords: Carbonylation; Metal–alkyl bonds; Organoiron complexes

Introduction

The conversion of carbon monoxide to carbon chains is certainly a highly rewarding reaction. This is done usually through heterogeneous catalysis based on the Fischer–Tropsch process. Insertion of surface-coordinated CO into a metal–alkyl bond is one of the supposed crucial steps of this process. The same insertion reaction has been reported to occur homogeneously within the coordination sphere of a metal centre [1–5]. A typical example is the complex (Cp)Fe(CO)$_2$CH$_3$ which can be transformed to a corresponding acyl derivative in a homogeneous reactor operating at high pressure of CO and temperature [6–8]. In spite of numerous studies of the carbonylation of CpFe-(CO)$_2$CH$_3$ and related complexes the detailed mechanism is not clear [9–12]. Alternatively, the same reaction is mediated by the activation of the metal–ligand bond by electron transfer [13]. Unlike a homogeneous reaction activated thermally, the electrochemical conversion of CpFe-(CO)$_2$CH$_3$ can be achieved at ambient temperature and atmospheric pressure, usually in the presence of a strong electron donating ligand (such as triphenyl phosphine PPh$_3$) [14]:

$$\text{CpFe(CO)}_2\text{CH}_3 + \text{PPh}_3$$
$$\xrightarrow{\text{e}^-} \text{CpFe(CO)(PPh}_3\text{)(CO}\cdot\text{CH}_3) \qquad (1)$$
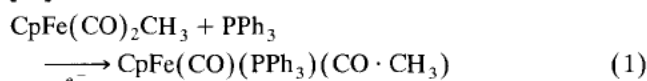
In the absence of an adequate ligand the acyl group formed by the bond insertion process migrates in the coordination sphere of iron leading to a substitution of the cyclopentadienyl ring [13]:

$$\text{CpFe(CO)}_2\text{(CH}_3)$$
$$\xrightarrow{\text{e}^-} (\text{CpCOCH}_3)\text{Fe(CO)(solv)}^- + \text{H}^+ \qquad (2)$$
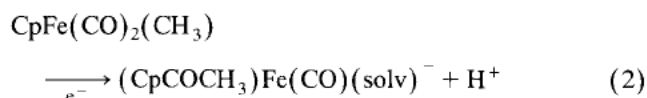
where "solv" denotes the solvent. Electrocatalytic preparative procedures have been described; however, no catalytic effect was observed in voltammetric experiments. This suggests that the electrochemical carbonylation reaction should involve an intricate interplay of processes with different time scales which allow the electrocatalysis to proceed in a preparative time scale but prevent its observation in a voltammetric time span [13]. The present work is intended to delineate such processes and to explain the role of intermediates participating in the overall electrocatalytic reaction.

. Experimental

The compound CpFe(CO)$_2$CH$_3$ was synthesized according to previously published procedures (Ref. [15] and

references therein). Triphenylphosphine (Aldrich) was of reagent grade. Tetrabutylammonium hexafluorophosphate or tetrafluoroborate used as supporting electrolytes were recrystallized and dried in vacuo. Tetrahydrofuran (THF), acetone and acetonitrile were purified by standard procedures [16]. The electrochemical measurements were made using a laboratory-built electrochemical system consisting of a fast rise time potentiostat and an interface to a personal computer (486,33 MHz) via an AD–DA card, PcLab model PCL818 (Advantech Co.). A three-electrode electrochemical cell was used with the Ag|AgCl|1 M LiCl reference electrode separated from the test solution by a salt bridge. One type of working electrode was a valve-operated static mercury electrode, SMDE2 (Laboratorní Přístroje, Prague). The voltage scan rate was synchronized with the formation of a fresh mercury drop electrode. The other working electrodes used in this study were gold mini- and microelectrodes with diameters 500 μm and 60 μm respectively. The auxiliary electrode was a cylindrical platinum net. Oxygen was removed from the solution by passing a stream of argon. Experiments were performed at 20 °C. The oxidation potential of ferrocene measured in the present arrangement was +0.700 V. In situ spectroelectrochemical measurements were made in a thin layer cell with a fine mesh platinum net in a three-electrode arrangement.

The cyclic staircase voltammetry was applied in its standard mode using a triangular voltage waveform and scan rates in the range from 50 mV s^{-1} to 240 V s^{-1}. The other type of voltammetric experiment used a trapezoidal shape of imposed voltage scan. In this mode, the electrode potential was scanned to a selected value in the diffusion-limited region where the potential was held for 10 s ± 0.5 ms. The reverse voltage scan was made higher with a scan rate either the same as or than the forward sweep. This "trapezoidal voltammetry" combines the advantage of the fast reverse sweep and the accumulation of products at a selected constant potential.

. Results and discussion

Experiments described in the literature conclude that the electrochemical reduction initiates a catalytic cycle (1) even keeping the electrode potential at a value where the electrolysis is just beginning to take place [14]. The present approach will investigate the electrochemical properties of the parent complex (CpFe(CO)$_2$CH$_3$), the acyl derivative CpFe(CO)$_2$(COCH$_3$), their interaction during the redox process and the influence of the migrating ligand (CO) on the short-lived reaction intermediates participating in reactions (1) and (2). Emphasis will be given to the elucidation of reaction (2).

The electrochemical reduction of CpFe(CO)$_2$CH$_3$ proceeds as an irreversible one-electron reduction characterized by the voltammetric cathodic wave at −2.05 V (Fig.

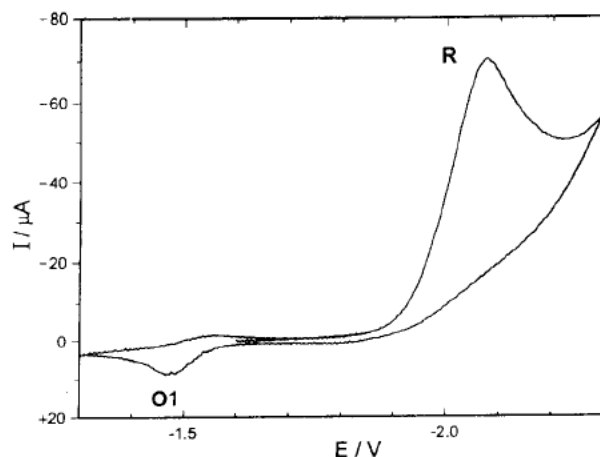Fig. 1. The cyclic voltammogram of 3.8 mM CpFe(CO)$_2$CH$_3$ and 0.1 M TBAPF$_6$ in acetone at a scan rate of 1 V s^{-1}. The initial potential was −1.6 V.

1). The voltammetric pattern is not influenced by the choice of solvent, the electrode material or the presence of a phosphine ligand. Nevertheless, the IR spectrum obtained on an optically transparent electrode in the presence of PPh$_3$ indicates that the complex loses one CO ligand (see the decrease in bands at 2005 cm^{-1} and 1947 cm^{-1} in Fig. 2 and growth of a new band at 1916 cm^{-1} corresponding to a single terminal CO group). Simultaneously a new band at 1610 cm^{-1} appears which is ascribed [12,15] to a coordinated acyl ligand (The reduction of CpFe(CO)$_2$CH$_3$ by a sodium amalgam in the presence of PPh$_3$ yields CpFe(CO)(PPh$_3$)(COCH$_3$) ($M = 454$), as proved by mass spectra containing the following lines: $m/e = 455$ (M + H), 411 (M + H–COCH$_3$), 383 (M +
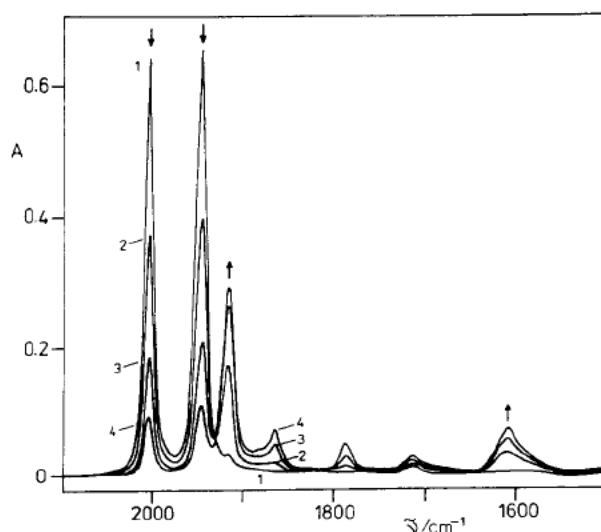

Fig. 2. The Fourier transform IR (FTIR) spectra of 1.6 mM CpFe(CO)$_2$CH$_3$, 5.7 mM PPh$_3$ and 0.1 M TBABF$_4$ in THF at the Pt minigrid electrode held at a potential of −1.65 V prior to the reduction. The time interval between measurements was 0 min (spectrum 1), 6 min (spectrum 2), 12 min (spectrum 3) and 18 min (spectrum 4).

H–2COCH$_3$), 428 (M + NH$_3$–COCH$_3$) and 400 (M + NH$_3$–2COCH$_3$).). It is sufficient to polarize the electrode on which the spectral changes are observed at a potential about 0.25 V more positive than the potential of the voltammetric wave, which suggests the participation of a catalytic process according to Eq. (1), triggered by the heterogeneous electron transfer.

Since the IR data confirmed the loss of one Fe–CO bond during the reaction, we considered it important to investigate the influence of free CO on the dissociation equilibria involved. The catalytic nature, hidden in the almost featureless voltammetric wave in Fig. 1, can be deduced from the influence of dissolved CO on the magnitude of voltammetric currents, as will be shown below. The voltammetry of fresh solutions of CpFe(CO)$_2$CH$_3$ in the absence of CO exhibits an anodic oxidation wave at − 1.45 V (denoted by O1) that is apparently too small with respect to the reduction wave R. However, taking into account the diffusion, one can estimate that the wave O1 represents the conversion of about 60% of the reduced parent complex. An experiment in which the product was accumulated is shown in Fig. 3 and confirms that the anodic wave O1 is due to a new reversible redox couple O1|R1, formed in a follow-up reaction to the reduction
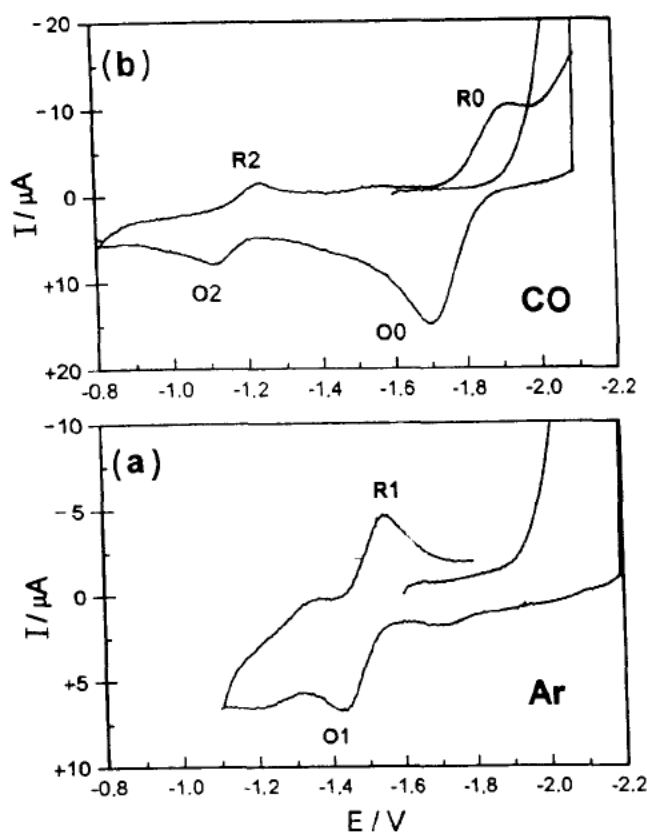

Fig. 4. The dependence of the ratio of anodic and cathodic current peaks on the scan rate. The solution was 4.2 mM CpFe(CO)$_2$CH$_3$ and 0.1 M TBAPF$_6$ in acetone under the atmosphere of argon (●, ▲) or under the atmosphere of CO (⊕). The curves are labelled with the corresponding peak potentials of the waves O0 and O1. ○, data obtained for the independent reduction of an authentic sample of CpFe(CO)$_2$(COCH$_3$) under the atmosphere of CO (see the text).

Fig. 3. The cyclic voltammetry of 3.7 mM CpFe(CO)$_2$CH$_3$ and 0.1 M TBAPF$_6$ in acetone with 10 s accumulation at the negative switching potential under atmospheres of (a) argon and (b) carbon monoxide. The scan rate was 61 V s^{-1}. The main reduction peak is off the scale.
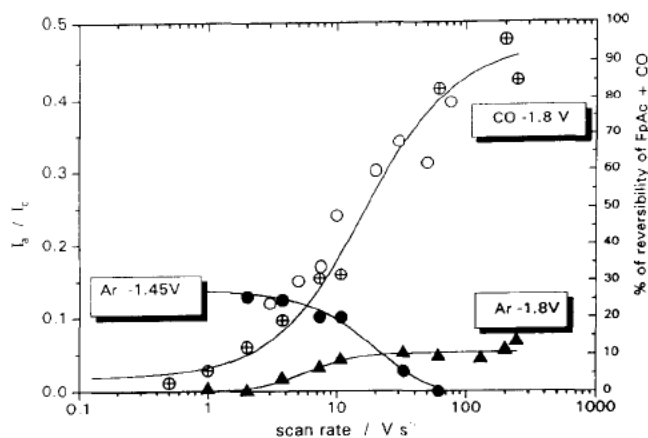
process R. When a similar experiment is performed in solution saturated with dissolved CO (Fig. 3(b)), another reversible system O0|R0 (at − 1.8 V) is generated (a small anodic wave identical to O0 can also be observed under inert atmosphere but only at very fast scan rate (see data in Fig. 4)), instead of the formation of the reversible redox couple O1|R1 (observed only under argon). The redox potential of the O0|R0 couple is identical with the reversible potential of the compound CpFe(CO)$_2$(COCH$_3$). The lifetime of both redox pairs generated by an EC process can be estimated from voltammetric currents measured at various scan rates (Fig. 4). Our data show unambiguously that the formation of CpFe(CO)$_2$(COCH$_3$) can be traced only as an intermediate by using fast scan voltammetry and that the yield is considerably enhanced by the presence of free CO. This finding seems to contradict the previously established experience that a long-term electrolysis yields the acyl compound, while its formation cannot be seen in the voltammetric time scale. Evidently, the mechanism of the electrochemical CO insertion reaction is a complicated process involving several other intermediates whose detection is difficult in routine experiments.

The observation of CpFe(CO)$_2$(COCH$_3$)$^{-\cdot}$ (wave O0 in Fig. 3(b)) only at short time scales (Fig. 4) was unexpected. Indeed, the redox couple of waves R0|O0 (at − 1.80 V, Fig. 5(a)) is almost perfectly chemically reversible even at long time scales. So it is a puzzling effect that CpFe(CO)$_2$(COCH$_3$)$^{-\cdot}$ could be formed in the initial stages of the reaction, that is at short time scales (Fig. 5(a)), but vanishes at a longer time scale. This evidence suggests the following: CpFe(CO)$_2$(COCH$_3$)$^{-\cdot}$ is stable under conditions where it is produced alone; however, it becomes unstable at long time scales when it encounters
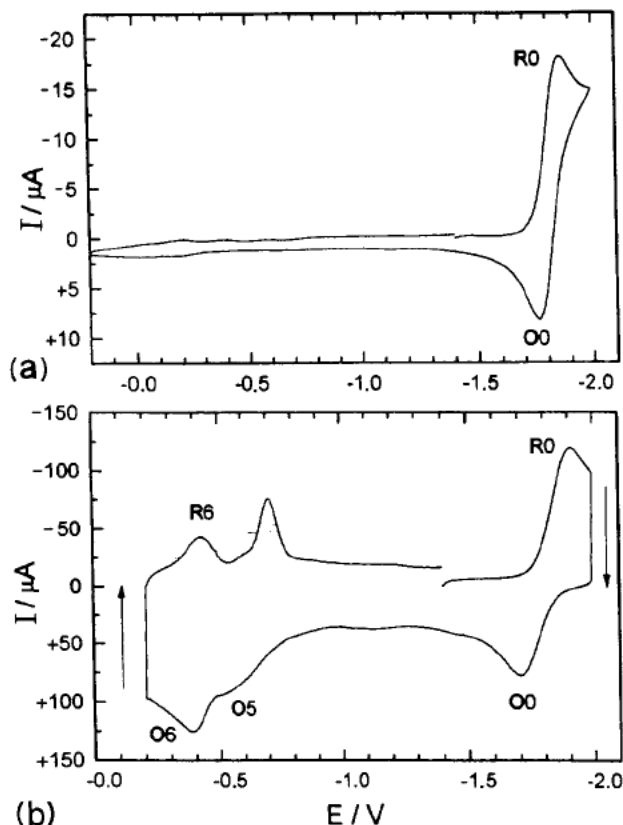
Fig. 6. The cyclic voltammetry of 1 mM $(Cp)Fe(CO)_2(COCH_3)$ and 0.1 M $TBAPF_6$ in THF ($– – –$) and in the presence of two equivalents of $CpFe(CO)_2CH_3$ (———). The scan rate was 0.1 V s^{-1}.

Fig. 5. The cyclic voltammetry of 0.8 mM $(Cp)Fe(CO)_2(COCH_3)$ and 0.1 M $TBAPF_6$, acetone. (a) Measured using the triangular waveform with sweep rate 1 V s^{-1} and the initial potential -1.4 V. (b) Measured at the scan rate 61 V s^{-1} and using two accumulation periods, each of 10 s duration, at potentials of -2.0 V (formation of reduction products) and -0.2 V (reoxidation of products).

electron transfer between $CpFe(CO)_2(COCH_3)^{-\cdot}$ and $CpFe(CO)_2CH_3$ is too slow to account for the decay of $CpFe(CO)_2(COCH_3)^{-\cdot}$ in the range of a few tens of volts per second, as observed in Fig. 4. The value of the rate constant k_{et} of the homogeneous electron transfer reaction was estimated to be 3200 M^{-1} s^{-1}. The observed decay has to include yet another reaction.

The problem of the acyl transfer reaction (2) [13] imposes the question of at which stage the metal-bound acyl migrates to the Cp ring. One can prove the existence of such a process by in situ FTIR spectroscopy (Fig. 7). The solution of $CpFe(CO)_2CH_3$ yields two absorption bands of CO vibrations at 2005 cm^{-1} and 1947 cm^{-1}. By scanning the electrode potential slowly, a gradual decrease in these bands is observed and two new, less intense bands at 1866 cm^{-1} and 1788 cm^{-1} appear. The new bands correspond to two CO ligands in the reduced complex. In addition to these bands of coordinated CO group, two new

the presence of reactants, products or intermediates generated from $CpFe(CO)_2CH_3$ and CO.

A first tentative explanation can be based on the existence of a homogeneous electron transfer from $CpFe(CO)_2(COCH_3)^{-\cdot}$ to unreacted $CpFe(CO)_2CH_3$. Such a reaction could have a key role in the overall performance of the catalytic CO insertion [2–4]. The experimental test of the above hypothesis was done by investigation of the reduction current and the reversibility of $CpFe(CO)_2(COCH_3)$ in the presence of varied concentrations of $CpFe(CO)_2CH_3$. A typical result is shown in Fig. 6, where a substantial increase in the wave of $CpFe(CO)_2(COCH_3)$ is concomitant with a loss of its reversibility. At high scan rate the homogeneous catalytic reduction is suppressed by a fast reoxidation of the radical anion during the reverse scan before the electron transfer to $CpFe(CO)_2CH_3$ could occur: the voltammetric pattern corresponds then to the sum of currents of both components and the reversible pair of redox waves of $CpFe(CO)_2(COCH_3)$ reappears. The experimental conditions for data in Fig. 6 (the mixture of $CpFe(CO)_2(COCH_3)$ and $CpFe(CO)_2CH_3$) cannot mimic fully the true situation corresponding to generation of such a mixture in situ (Fig. 4). Nevertheless, it appears that the

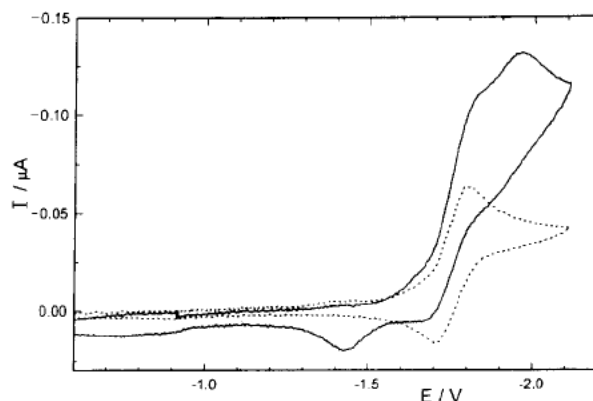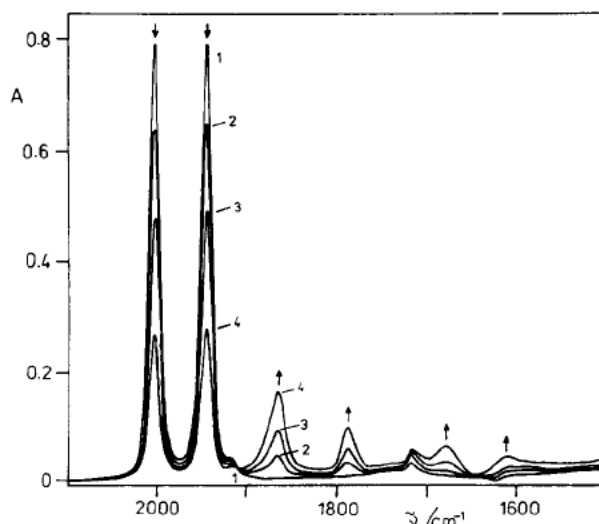Fig. 7. The FTIR spectra of 2.8 mM $CpFe(CO)_2CH_3$ and 0.1 M $TBABF_4$ in THF at different potentials of the Pt minigrid electrode: spectrum 1, 0 V; spectrum 2, -1.85 V; spectrum 3, -1.95 V; spectrum 4, -2.0 V. The time interval between measurements was 150 s.

bands associated with the migration of CO ligand can be seen. The band at 1679 cm^{-1} was ascribed in the literature to the vibration of a CO group attached to the cyclopentadienyl ring [17,18]. The slightly less intense band at 1610 cm^{-1} corresponds to the vibration of acyl group –COCH$_3$ coordinated to iron. The CO vibration of the acyl ligand is characterized by much lower wavenumbers than expected for a keto group owing to interaction with d orbitals of the metal. Two limiting forms of CO have the double bond either between carbon and oxygen or between carbon and metal resulting in an average configuration characterized by lower vibration frequency compared with organic aldehydes or ketones [12].

The process of acyl migration from the iron atom to Cp ligand requires one to reconsider the stability of the CpFe-(CO)$_2$(COCH$_3$) complex in the reduced state. A meticulous inspection of the voltammogram of CpFe(CO)$_2$-(COCH$_3$) reveals a certain possibility of formation of products reoxidized at about –0.4 V. Because of a large voltage span between the wave of CpFe(CO)$_2$-(COCH$_3$) and that of additional products, diffusion renders the detection of possible products rather difficult. This obstacle was resolved by application of "trapezoidal" voltammetry (i.e. holding the potential scan for the sake of accumulation of products at a suitable potential). Fig. 5(b) proves that the reduction of CpFe(CO)$_2$(COCH$_3$) is an EC process generating two intermediates with reoxidation potentials of approximately –0.5 and –0.4 V. The appearance of a reversible redox couple at –0.4 V correlates well with the reoxidation waves observed in solutions of CpFe(CO)$_2$CH$_3$ subjected to a non-exhaustive electrolysis (Fig. 8). The partially electrolysed solution exhibits a wave at –0.32 V, ascribed [9] to (CH$_3$COCp)Fe(CO)$_2$ anion. Another small wave is observed at –0.1 V that may correspond to free substituted CpAcyl ligand in the form of an anion. Acylcyclopentadienide anion is very difficult to prepare; however, its electrochemical in situ generation
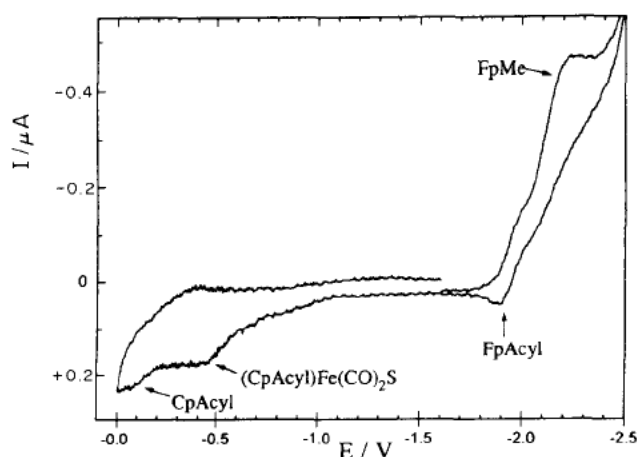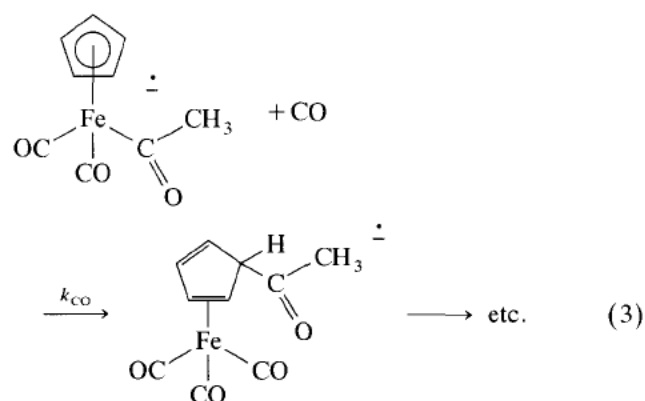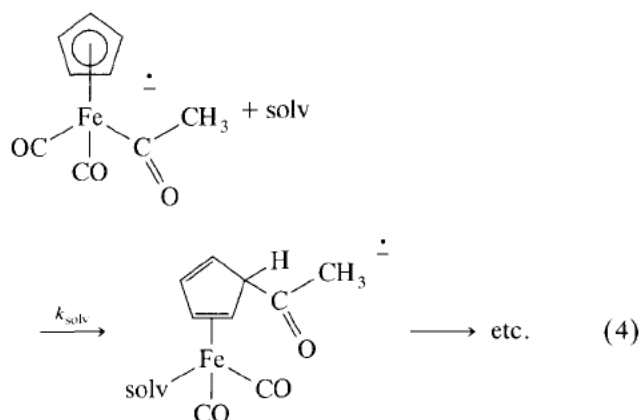
was successful [10]. Its anodic oxidation potential was reported to be identical with that of the wave at –0.1 V found here. Considering the FTIR data described above, it can be concluded that the acyl-substituted Cp ligand partially dissociates during the electrolysis.

At this stage it appears that CpFe(CO)$_2$(COCH$_3$)$^{-\cdot}$ is intrinsically unstable when it is subjected to the reaction conditions that resemble its formation from CpFe(CO)$_2$CH$_3$ and CO. Under the conditions of Fig. 5(a), this intrinsic instability is suppressed because the concentration of the intermediates in the diffusion layer is small. However, when more products are accumulated, as in Fig. 5(b), this instability is revealed by the large height of the waves O5 and O6. Since we know (i) that the ultimate products correspond to a migration of the acyl group to the Cp ring (see the IR spectra above and the voltammetry of partially electrolysed solution in Fig. 8) and (ii) that CO is released during the reduction of CpFe(CO)$_2$CH$_3$ (see IR and Fig. 2), one can suppose that the migration of the acyl group is enhanced in the presence of CO. Thus CpFe(CO)$_2$-(COCH$_3$)$^{-\cdot}$ would be stable when it is produced alone because no CO ligand is available to promote the migration of acyl group to the Cp ring. However, it becomes unstable when such a ligand is present. This mechanistic assumption was tested in the following experiment. The reversible voltammetry of CpFe(CO)$_2$(COCH$_3$) was scrutinized under the atmosphere of CO. The presence of an excess of the CO ligand causes a very efficient consumption of CpFe(CO)$_2$(COCH$_3$)$^{-\cdot}$ via a follow-up chemical reaction leading to a voltammetric irreversibility at lower scan rates. At high scan rates this chemical process is suppressed and the reversibility of voltammetric wave is restored. The corresponding data are shown in Fig. 4 (open circles). It is noteworthy that these data coincide with those relative to CpFe(CO)$_2$(COCH$_3$)$^{-\cdot}$ generated during the reduction of CpFe(CO)$_2$CH$_3$ (cross-centred circles). One can then safely conclude that in both cases the same kinetics are involved. This reaction plays a key role in the overall reaction scheme (discussed in the last section) because it identifies the main termination reaction of the catalytic cycle. The CO-promoted migration mechanism is characterized by the pseudo-first-order homogeneous rate constant k_{co}[CO] which was estimated to be 50 s^{-1}.

Fig. 8. The cyclic voltammetry of partially (40%) electrolysed solution of initial concentration 4 mM CpFe(CO)$_2$CH$_3$ + 0.1 M TBABF$_4$ in acetone at Au microelectrode at 1 V s^{-1}.

(3)

$$\xrightarrow{k_{solv}} \quad \longrightarrow \text{ etc.} \quad (4)$$

This also logically explains why the stability of CpFe(CO)$_2$(COCH$_3$)$^{-\cdot}$ is about 10 times higher when it is generated by the reduction of CpFe(CO)$_2$CH$_3$ under the argon atmosphere than under the atmosphere of CO (compare in Fig. 4 the data marked by full triangles and crossed circles). The simultaneous existence of reactions (3) and (4) may explain all the above observations. When the reduction of CpFe(CO)$_2$(COCH$_3$) alone is performed (Fig. 5) only the relatively slow reaction (4) would play a role leading to the observation of an almost chemically reversible voltammetry. When CpFe(CO)$_2$(COCH$_3$)$^{-\cdot}$ is produced by reduction of CpFe(CO)$_2$CH$_3$ under an argon atmosphere, a small steady state concentration of CO is present in the diffusion layer that is supplied by the fragmentation of the 19-electron CpFe(CO)$_2$CH$_3^{-\cdot}$ (Fig. 4, data marked by full triangles). In this respect it must be noted that the increase in the wave O1 (Fig. 4, full circles) is concomitant with the decrease in the wave O0 (CpFe(CO)$_2$(COCH$_3$)$^{-\cdot}$, full triangles in Fig. 4):

$$\longrightarrow \quad + \text{ CO} \quad (5)$$

$$\text{CO} + \quad \xrightarrow{k_{CO}} \quad (3)$$
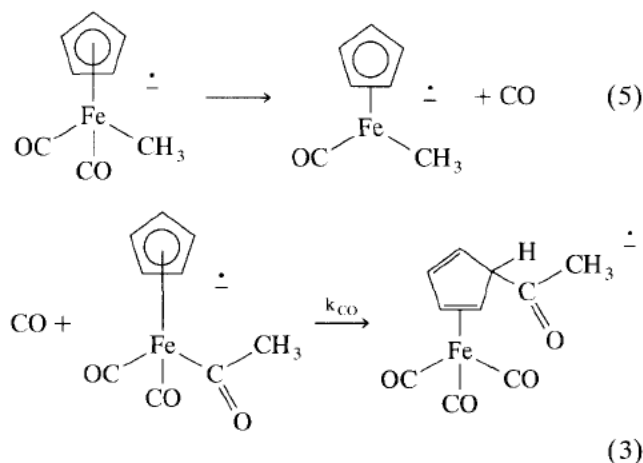
When the reduction of CpFe(CO)$_2$CH$_3$ is performed under an excess of CO, reaction (3) is even more dominant because the concentration of CO in the diffusion layer is much larger. As a result the decay of CpFe(CO)$_2$(COCH$_3$)$^{-\cdot}$ occurs at higher scan rates.

Reaction mechanism

On the basis of experimental observations described above, the competitive and catalytic reactions participating in the overall electrochemical activation of CpFe(CO)$_2$CH$_3$ can be described by Scheme 1. The potentials in Scheme 1 are assigned tentatively with respect to the experimental conditions used in this study). The electrochemical one-electron reduction of CpFe(CO)$_2$CH$_3$ yields a highly unstable form CpFe(CO)$_2$CH$_3^{-\cdot}$ that chemically decomposes by at least three reaction pathways. The principal reactions are the loss of CO ligand and the insertion of CO into the metal–methyl bond. The first reaction leads to CpFe(CO)(solv)Me$^{-\cdot}$ (where solv is the solvent) giving the reoxidation wave at -1.45 V. The second reaction yields CpFe(CO)(solv)(COCH$_3$)$^{-\cdot}$ which can be stabilized by trapping CO released in the first reaction path or supplied by the atmosphere of CO ligand or by added phosphine. (The reoxidation of CpFe(CO)(solv)(COCH$_3$)$^{-\cdot}$ probably proceeds in a wave O2 at -1.2 V. O2 has a transient character and is enhanced by the presence of CO (e.g. under the conditions when the first pathway is suppressed). O2 can also be observed in high resolution voltammograms as a product of a direct reduction of CpFe(CO)$_2$(COCH$_3$) in the absence of CpFe(CO)$_2$CH$_3$.) If a strong electron donating phosphine ligand is present the main product of the large-scale electrolysis is CpFe(CO)(PR$_3$)(COCH$_3$), as described in the literature [19]. Without an external supply of CO the stabilization is not very efficient, owing to the small steady state concentration of CO. Once the acyl derivative is formed, it is capable of reducing CpFe(CO)$_2$CH$_3$ in a homogeneous reaction and in this way triggering the electrocatalytic cycle.

By analogy the with properties of the unstable CpFe(CO)$_2$CH$_3^{-\cdot}$ radical anion, the 19-electron intermediates CpFe(CO)$_2$(COCH$_3$)$^{-\cdot}$ and CpFe(CO)(solv)(COCH$_3$)$^{-\cdot}$ are expected to have a similar instability, causing the slippage of the Cp ring to η^4 configuration and the migration of the acyl group. The change in the coordination of the Cp ligand is a prerequisite to the migration of the acyl group to the Cp ring (observed here in IR spectra). Similar migration of a group from the central transition metal atom to the Cp ring is well established in several other organometallic reactions [20–23]. A very similar process of the migration of acyl group was found during an attempted acylation of (η^5-cycloheptadienyl)-Fe(CO)$_2$CH$_3$ complex.

The reactivity of the anion radical CpFe(CO)$_2$(COCH$_3$)$^{-\cdot}$ plays a crucial role (as important as the reactivity of CpFe(CO)$_2$CH$_3^{-\cdot}$) in the propagation of the catalytic cycle. Moreover, it explains the discrepancy between the products obtained in preparative electrolysis (i.e. catalysis) and in voltammetry. CpFe(CO)$_2$(COCH$_3$)$^{-\cdot}$ participates in two main reactions: (i) the redox exchange with CpFe(CO)$_2$CH$_3$ (e.g. the propagation) and (ii) the
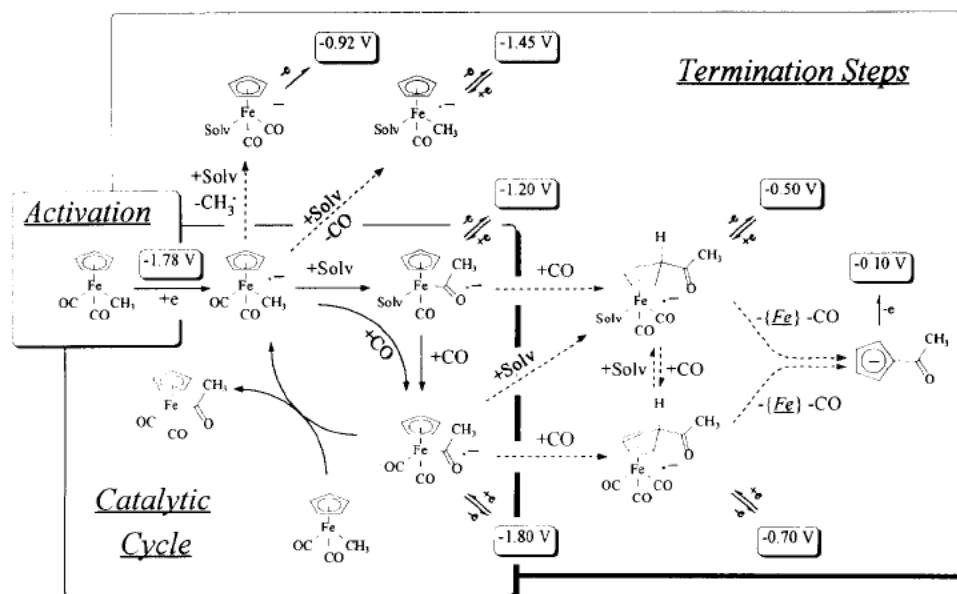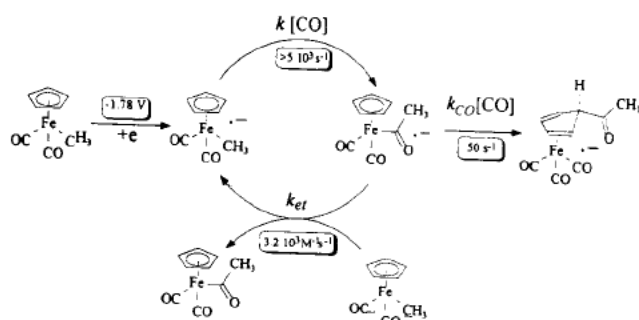
Scheme 1.

migration of the acyl group promoted by CO (e.g. termination steps), which are shown in a simplified Scheme 2. Data in Fig. 4 indicate that the CO-assisted formation of $CpFe(CO)_2(COCH_3)$ is time independent above 200 V s^{-1}, affording an estimate of the lower limit of the pseudo-first-order rate constant for the CO insertion–addition reaction to values $k[CO] > 5000$ s^{-1}. The estimated values of $k_{et} = 3200$ M^{-1} s^{-1} and $k_{co}[CO] = 50$ s^{-1} allow us to calculate the maximal conversion efficiency of each catalytic cycle by

$$p_{max} = \frac{k_{et}[FpMe]}{k_{et}[FpMe] + k_{co}[CO]} = \frac{1}{1 + 15.6/[FpMe]} \quad (6)$$

where $[CpFe(CO)_2CH_3]$ is in millimolar units. A typical electropreparation may use $[CpFe(CO)_2CH_3] = 100$ mM that allows us to achieve 86% efficiency for each cycle, while a voltammetric experiment using $[CpFe(CO)_2CH_3] = 1$ mM is performed only at 6% efficiency and therefore the catalytic effects cannot be routinely observed. These numbers are maximum values for each cycle since we have identified other termination processes (see Scheme

1). Among these, several, not fully identified in the present study, produce additional small anodic waves located between -0.6 and -1.0 V: O3 (-0.92 V) and O4 (-0.70 V) which may further lower the real efficiency of the whole process.

References

[1] R.H. Marguson, R. Meirowitz, S. Zulu and W.P. Giering, Organometallics, 2 (1983) 460.
[2] J.P. Colleman, Acc. Chem. Res., 8 (1975) 342.
[3] M.P. Cooke, Jr., J. Am. Chem. Soc., 92 (1970) 6080.
[4] C.P. Casey, R.A. Widenhoefen and J.M. O'Connor, J. Organomet. Chem., 428 (1992) 99.
[5] M.J. Wax and R.G. Bergman, J. Am. Chem. Soc., 103 (1981) 7028.
[6] T.C. Forschner and A.R. Cutler, Organometallics, 4 (1985) 1247.
[7] R.B. King, A.D. King, Jr., M.Z. Igbal and C.C. Frazier, J. Am. Chem. Soc., 100 (1978) 1687.
[8] R.S. Su and A. Wojciki, J. Organomet. Chem., 87 (1971) 231.
[9] M. Green and D.J. Westlake, J. Chem. Soc. A, (1971) 367.
[10] I.S. Butler, F. Basolo and R.G. Pearson, Inorg. Chem., 6 (1967) 2074.
[11] A.J. Hart-Davis and R.J. Mawby, J. Chem. Soc. A, (1969) 2403.
[12] R.B. King, J. Am. Chem. Soc., 85 (1963) 1919.
[13] D. Miholová and A.A. Vlček, Proc. 10th, Conf. on Coordination Chemistry 1985, p. 275.
[14] D. Miholová and A.A. Vlček, J. Organometal. Chem. 240 (1982) 413.

Scheme 2.

[15] R.B. King, in J.J. Eisch and R.B. King (eds.), Organometallic Synthesis, Vol. 1, Academic Press, New York, 1965, p. 175.

[16] J.A. Riddick and W.B. Bunger, Organic Solvents, Wiley Interscience, New York, 1970, p. 572.

[17] N. El Murr and A. Chaloyard, J. Organomet. Chem., 193 (1980) C60.

[18] A. Chaloyard and N. El Murr, Inorg. Chem., 19 (1980) 3217.

[19] D. Miholová and A.A. Vlček, Inorg. Chim. Acta, 43 (1080) 43.

[20] S.R. Beryhill and B. Sharenow, J. Organomet. Chem., 221 (1981) 143.

[21] S.R. Beryhill, G.L. Clevenger and F.Y. Burdurlu, Organometallics, 4 (1985) 1509.

[22] G. Fachinetti, S.D. Nero and C. Floriani, J. Chem. Soc., Dalton Trans., (1976) 203.

[23] F.W.S. Benfield and L.M.H. Green, J. Chem. Soc., Dalton Trans., (1974) 1324.

[24] M.W. Gregory, R.A. Fisher and R.A. Heyn, Organometallics, 5 (1986) 818.